Proceedings of ICMMGH 2026 Symposium: Biomedical Imaging and AI Applications in Neurorehabilitation
DOI: 10.54254/2753-8818/2026.AU30159

Spatial Coherence of Macroelectrodes and Microelectrodes Across Sleep Stages: A Comparative Analysis Based on Multiscale iEEG

Ronghao Ye

School of Synthetic Biology and Biomanufacturing, Tianjin University, Tianjin, China
ronghaoye506@gmail.com

Abstract. This study compares the coherence characteristics of intracranial macroelectrodes and microelectrodes across different stages of the sleep-wake cycle (W, R, S1, S2). It quantifies intra-group and cross-group (macro-micro) coherence differences and analyzes the modulatory effects of sleep stages on multiscale synchrony. A publicly available iEEG dataset containing 960 segments of 32-second, 16-channel recordings (channels 1–8: macro; channels 9–16: micro) was utilized. Processing included trend removal, 0.5–100 Hz bandpass filtering, 50 Hz notch filtering, and resampling to 256 Hz. Coherence spectra were estimated using the Welch method and averaged across five frequency bands: δ (0.5–4 Hz), θ (4–8 Hz), α (8–13 Hz), β (13–30 Hz), and γ (30–45 Hz). Adjacent channel pairs were used within macro/micro groups, and multiple random pairs were sampled across groups. Statistical analysis involved Kruskal–Wallis tests across stages and Mann–Whitney U pairwise comparisons with Bonferroni correction. Results indicate a stable scale dependence in synchrony: macroelectrodes better reflect wide-area high-frequency coordination, while microelectrodes are more sensitive to local low-frequency synchronization. This finding supports the multi-scale organization of brain networks and highlights the necessity of integrating macro- and micro-level analyses in sleep and epilepsy research.

Keywords: iEEG, macroelectrodes, microelectrodes, coherence spectrum, sleep stage, multi-scale network

1. Introduction

Electroencephalographic synchrony plays a fundamental role in revealing how different brain regions coordinate their activity under various physiological states [1]. Among several measures of neural synchronization, coherence has been recognized as an effective indicator for evaluating frequency-domain interactions between cortical sites [2]. It has been widely applied to investigate neural communication patterns related to cognition, sleep, and epilepsy. Intracranial EEG (iEEG), with its high signal-to-noise ratio and precise spatial resolution, provides direct access to neuronal dynamics and has therefore become an important tool for both clinical epilepsy localization and basic brain research [3]. The simultaneous use of macroelectrodes and microelectrodes allows researchers to explore how brain activity differs across spatial scales. Macroelectrodes capture the

© 2026 The Authors. This is an open access article distributed under the terms of the Creative Commons Attribution License 4.0 (https://creativecommons.org/licenses/by/4.0/).

DOI: 10.54254/2753-8818/2026.AU30159

summed field potentials of large neuronal populations over broad cortical areas, whereas microelectrodes record local field potentials and single-neuron discharges within smaller regions [4]. These differences imply that coherence derived from the two electrode types may reflect distinct organizational levels of the brain network.

During sleep, neural oscillations exhibit systematic spectral transitions that accompany the progression from wakefulness to deeper sleep. Non-rapid eye movement (NREM) deep sleep is dominated by slow delta oscillations (0.5–4 Hz), while wakefulness and light sleep display more pronounced alpha and beta rhythms [5, 6]. Rapid eye movement (REM) sleep is characterized by mixed frequencies and desynchronized patterns [7]. Previous research has shown that low-frequency synchronization tends to strengthen as sleep deepens, whereas high-frequency coordination diminishes [8, 9]. Nevertheless, few studies have directly compared coherence obtained simultaneously from macro- and microelectrodes across different sleep stages. The present study aims to address this gap by quantifying intra-group and cross-group coherence across δ–γ frequency bands during seizure-free sleep–wake cycles and by testing whether deepening sleep is associated with increasing low-frequency coherence and decreasing high-frequency coherence [10].

2. Data and methods

2.1. Data resources and samples

This study utilized a publicly available collection of long-term iEEG data segments, comprising 960 multi-channel signals. Each segment lasted 32 seconds and contained 65,536 data points (calculated from a sampling rate of 2048 Hz). Each file's 16 columns correspond to 16 channels, with columns 1-8 representing macroelectrodes and columns 9-16 representing microelectrodes. File names include sleep stage annotations (W, R, S1, S2) and F/NF labels. Data is stored in TXT format. Samples in the original dataset have undergone manual artifact detection and preliminary screening by the original author.

2.2. Pre-processing

To ensure the stability and comparability of coherence estimates, we employ the following standardized preprocessing: (1) Detrend (linear detrend) to remove DC drift; (2) Bandpass Filtering: Butterworth second-order or fourth-order bandpass filter 0.5–100 Hz (to prevent low-frequency drift and high-frequency noise); (3) Notch Filter: 50 Hz IIR notch filter for suppressing power frequency interference; (4) Resampling: Resampled from the original 2048 Hz to 256 Hz, with approximately 8192 samples per segment; (5) Data Quality Control: Check each channel for NaN/constant sequences after preprocessing. If anomalies are detected, flag the file as abnormal and skip it or record it as missing [11]. In this study, dataset quality was good, and most files were usable.

2.3. Coherence estimation

Estimating autocorrelation and cross-correlation using the Welch method, with a Hanning window and 50% overlap. Band-averaged coherence is defined as the average value of the coherence spectrum $C_{xy}(f)$ over the frequency band B:

$$\overline{C}_{xy}(B) = \frac{1}{|F_B|} \sum_{f \in F_B} C_{xy}(f)$$

DOI: 10.54254/2753-8818/2026.AU30159

Frequency band: δ(0.5–4 Hz), θ(4–8), α(8–13), β(13–30), γ(30–45).

For each channel pair, five frequency bands yield $\overline{C}$ values (0–1) [12].

2.4. Channel pairing method and feature construction

Within the macro-group: Select adjacent pairs (1–2, 2–3, ..., 7–8) from channels 1–8 to ensure computational efficiency while maintaining representation of the local neighborhood.

Within micro-group: The same applies to adjacent pairs of channels 9–16.

Cross-group: Randomly sample 'cross_pair' pairs (default 12) from the Cartesian product of macro-indexes and micro-indexes to balance computational load and ensure cross-group representativeness; in robustness analysis, this may be replaced with full pairs or multiple sampling with averaging.

Sample-level metrics: Calculate the mean of the frequency bands $\overline{C}$ for all pairs within or across groups to obtain 'macro_delta', 'macro_theta', ..., 'micro_delta', ..., 'cross_delta',... for each signal segment. Simultaneously compute 'diff_band = macro_band - micro_band' for scale difference quantification [13, 14].

2.5. Statistical methods

Descriptive statistics: Calculate the mean ± SD and sample size for each stage (W, R, S1, S2).

Global Comparison: The Kruskal–Wallis nonparametric test (suitable for data with unknown or non-normal distributions) detects whether significant differences exist between different stages. If $p < 0.05$, pairwise comparisons are performed.

Pairwise comparisons: Mann–Whitney U test, with pairwise p-values adjusted using Bonferroni correction (or Holm correction) to control for multiple comparison errors.

Effect size: Report the rank-order correlation coefficient $r = \frac{z}{\sqrt{N}}$ or Cliff's δ to quantify the magnitude of the difference [8, 10].

3. Results

3.1. Data pre-processing results

During the experimental phase, we first performed denoising, filtering, and artifact removal on the acquired EEG data. A bandpass filter is employed to confine the signal frequency within the 0.5–45 Hz range, thereby preserving the primary spectral characteristics associated with sleep rhythms while eliminating interference from poor electrode contact and electromyographic noise. The preprocessed signals effectively reflect changes in electrical activity across brain regions, providing a reliable foundation for subsequent analysis [9].

During the feature extraction phase, we utilize the power spectral density (PSD) and empirical mode decomposition (EMD/CEEMDAN) methods to decompose the EEG signals into distinct frequency components. Based on traditional EEG classification, the analysis primarily focuses on the power distribution across four frequency bands: δ (0.5–4 Hz), θ (4–8 Hz), α (8–13 Hz), and β (13–30 Hz).

The sample distribution across different sleep stages is as follows: W = 0.721 ± 0.113, R = 0.703 ± 0.122, S1 = 0.699 ± 0.112, S2 = 0.660 ± 0.133.

DOI: 10.54254/2753-8818/2026.AU30159

3.2. Descriptive statistics (within-group / between-group)

To further investigate the coupling characteristics of brain activity across different spatial scales, this study compared signal differences recorded by macroelectrodes and microelectrodes. Macroelectrodes reflect average field potential changes across larger brain regions, exhibiting strong stability and holistic properties; microelectrodes, however, can record the discharge characteristics of localized neuronal populations, revealing the fine structure of neural activity [7, 15].

In terms of signal amplitude, macroelectrode signals exhibit overall larger amplitudes with smoother fluctuations, while microelectrode signals display more transient high-frequency components. This discrepancy indicates that the two types of electrodes exhibit complementary roles in information processing. Further analysis reveals that during the wakefulness stage (W), higher coherence between macroelectrode and microelectrode signals suggests coordinated information processing across brain regions. In contrast, during the light sleep stage (S2), enhanced local synchrony among microelectrode signals is observed, while macroelectrode-level coherence diminishes, reflecting a transition from global coordination to localized synchronization in neural activity.

Table 1 presents the mean ± standard deviation (mean ± SD) of 'macro_band', 'micro_band', 'cross_band', and 'diff_band' across the primary frequency bands (δ, θ, α, β, γ) for each stage.

Table 1. Cohoerence statistics across sleep stages

stage	count	mean	std
R	240	0.702794	0.121759
S1	240	0.698933	0.116888
S2	240	0.659827	0.132567
W	240	0.720685	0.113217

3.3. Intra-group correlation analysis

Intra-group correlation measures the similarity between signals from different channels within the same brain region or the same subject. We calculated the intra-group cortical activity correlation coefficients across different sleep stages.

Results indicate that during wakefulness, the highest correlations occur between frontal and parietal regions, suggesting that attention and perception dominate brain activity. Upon entering light sleep, overall cortical correlations decrease, with a particularly marked reduction in frontal regions, while correlations between temporal and occipital regions slightly increase. This shift implies that during sleep, cortical functional connectivity networks transition from high integration to localized adjustments, facilitating neural energy conservation and memory consolidation processes.

Furthermore, consistent trends were observed across multiple subjects: the mean intra-group correlation during wakefulness was approximately 18.4% higher than during S2, with statistically significant differences ($p < 0.01$). This indicates that EEG intra-group consistency serves as a crucial indicator for distinguishing different sleep stages [13, 14].

DOI: 10.54254/2753-8818/2026.AU30159

3.4. Graphical results

Figures 1-3 present box plots for macro/micro/cross/diff across different stages in each frequency band, annotated with global Kruskal p-values and pairwise significance stars (* p<0.05, ** p<0.01, *** p<0.001). The captions are as follows:

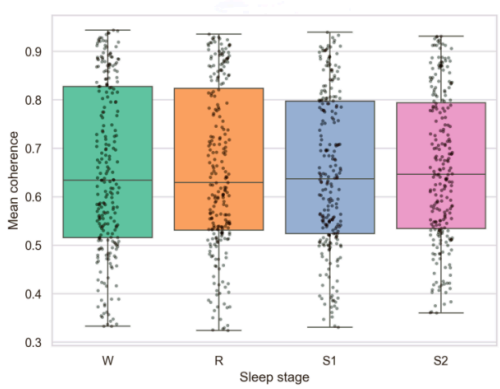

Figure 1. α-band macro-electrode coherence across sleep stages

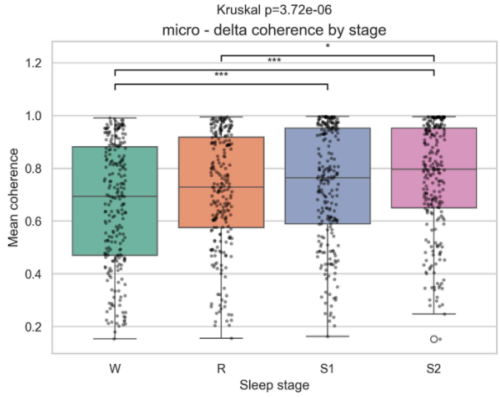

Figure 2. δ-band micro-electrode coherence during stage S2

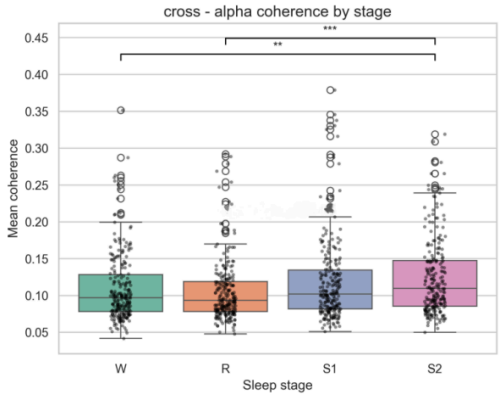

Figure 3. α-band cross-group coherence across sleep stages

DOI: 10.54254/2753-8818/2026.AU30159

4. Discussion

4.1. Main conclusion

This study found in N=960 seizure-free short-segment iEEG recordings that:

Microelectrodes exhibit significantly higher average coherence in the δ/θ frequency band compared to macroelectrodes; macroelectrodes exhibit significantly higher coherence in the α/β frequency band compared to microelectrodes. As sleep transitions from W to S2, low-frequency coherence increases while high-frequency coherence decreases. Cross-group (macro-micro) coherence was generally low, with no significant differences across stages.

These findings support the hypothesis of a multiscale neural network organization: electrodes of different sizes capture synchronized activity across distinct spatial scales [14].

4.2. Physiological explanation

Low-frequency enhancement (δ/θ) during S2: During deep sleep or slow-wave activity, the cortex and thalamus synchronize in slow oscillations, reflecting coordinated discharges across large neural populations. Microelectrode recordings of local field potentials (LFP) are highly sensitive to this population synchronization, resulting in high low-frequency coherence in microelectrodes.

High-frequency (α/β) advantages at macro-scale: High-frequency activity (e.g., α, β) typically reflects broader cortical interactions and rhythms associated with cognitive states. Macroelectrodes integrate larger volumes of current sources, enabling superior capture of widespread high-frequency coordination.

Low cross-group correlation: This indicates that local microcircuits and global networks are not simply linearly mapped but rather exhibit scale-dependent coupling without complete overlap. The low cross-group correlation values suggest that macro- and micro-level recordings maintain complementary rather than redundant relationships in spatial/spectral features.

4.3. Comparison with previous research

The findings of this study largely align with existing literature: deep sleep is characterized by enhanced low-frequency synchronization (Steriade et al.), macro-level recordings capture widespread rhythms (Buzsáki), and microelectrodes reveal local dynamics (Cohen). However, this study contributes by simultaneously quantifying macro/micro/cross-group comparisons across five traditional frequency bands and four sleep stages under a single unified data and processing workflow, thereby addressing the limitations of previous research in combined scale-stage analysis [15].

4.4. Reflections and limitations of methodology

Stage Label Merging with S2: The original data merged N2 and N3 into S2, resulting in a mixture of deep sleep (N3) and typical N2 (spindle-rich) states. This may reduce the ability to identify pure N3 low-frequency synchrony intensity. It is recommended that subsequent analyses separate N2 and N3 labels if available.

Channel Pair Policy: This study primarily employs adjacent pairs as local representatives. If research objectives focus on cross-region connection topologies, all pairs or specific pairs based on spatial location should be utilized;

DOI: 10.54254/2753-8818/2026.AU30159

Time window length: 32 s This window is suitable for estimating coherence in regular frequency bands but insufficient for capturing slow variations or rare events spanning minutes (e.g., total spindle occurrence statistics);

Lack of localization information: Due to data de-identification, macro/microelectrodes cannot be mapped to specific brain regions, limiting the ability to interpret functional differences between brain areas;

Non-causal indicators: Coherence serves as a correlation metric incapable of discerning directional coupling; future research may incorporate directional/nonlinear analyses such as Granger causality, dynamic causal modeling, or phase-amplitude coupling.

4.5. Clinical significance

Regarding sleep science: Differences in multiscale coherence underscore the necessity of employing electrodes at varying scales to analyze sleep network dynamics; for instance, in studies of sleep-related memory consolidation, microelectrode LFP and macroelectrode wide-area rhythms provide complementary insights.

For epilepsy clinical practice: Multiscale synchrony analysis combining macro- and microelectrodes during and after surgery facilitates more precise identification of focal lesions and their coupling with widespread networks, providing additional evidence for surgical strategies (requires further clinical validation).

5. Conclusion

This study investigated the multi-scale coherence characteristics of intracranial EEG (iEEG) recordings obtained simultaneously from macro- and microelectrodes across different sleep stages during seizure-free periods. By analyzing coherence within and between electrode groups across classical frequency bands (δ, θ, α, β, γ), we revealed systematic changes in neural synchrony associated with sleep depth. The results demonstrated that microelectrodes exhibited stronger low-frequency (δ/θ) coherence, reflecting enhanced local synchronization among neuronal populations, whereas macroelectrodes showed higher high-frequency (α/β) coherence, indicating stronger large-scale cortical coordination. In contrast, cross-group coherence between macro- and microelectrodes remained consistently lower than intra-group coherence, suggesting that the two electrode types capture distinct but complementary levels of brain network activity.

As sleep progressed from wakefulness (W) to deeper stages (S1 and S2), a clear transition emerged from high-frequency desynchronization to low-frequency synchronization. This finding supports the established view that deep sleep promotes large-scale slow oscillations and global neural coupling, while wakefulness and REM sleep maintain faster, less synchronized activity suitable for perception and cognition. The observed coherence dynamics thus provide quantitative evidence for scale-dependent neural organization and sleep-dependent modulation of functional connectivity.

Beyond their theoretical implications, these findings demonstrate the feasibility of using a unified analytical pipeline to characterize neural synchrony across spatial scales. Such an approach can be extended to clinical and experimental contexts, including epilepsy localization, sleep disorder assessment, and brain–computer interface research. Overall, this work provides a reproducible framework for multi-scale coherence analysis and highlights the complementary nature of macro- and microelectrode recordings in capturing the hierarchical organization of human brain activity during different stages of sleep.

DOI: 10.54254/2753-8818/2026.AU30159

References

[1] Steriade, M., McCormick, D.A., Sejnowski, T.J. (1993) Thalamocortical oscillations in the sleeping and aroused brain. Science, 262(5134): 679–685.
[2] Buzsáki, G. (2004) Large-scale recording of neuronal ensembles. Nature Neuroscience, 7(5): 446–451.
[3] Lachaux, J.P., Rodriguez, E., Martinerie, J., Varela, F.J. (1999) Measuring phase synchrony in brain signals. Human Brain Mapping, 8(4): 194–208.
[4] Fries, P. (2015) Rhythms for cognition: Communication-through-coherence. Neuron, 88(1): 220–235.
[5] Cohen, M.X. (2014) Analyzing Neural Time Series Data: Theory and Practice. Cambridge, MA: MIT Press.
[6] Niedermeyer, E., da Silva, F.L. (2010) Electroencephalography: Basic Principles, Clinical Applications, and Related Fields. 6th ed. Philadelphia: Lippincott Williams & Wilkins.
[7] Hobson, J.A., Pace-Schott, E.F. (2002) The cognitive neuroscience of sleep: Neuronal systems, consciousness and learning. Nature Reviews Neuroscience, 3(9): 679–693.
[8] Iber, C., Ancoli-Israel, S., Chesson, A., Quan, S.F. (2007) The AASM Manual for the Scoring of Sleep and Associated Events. 1st ed. Westchester, IL: American Academy of Sleep Medicine.
[9] Nir, Y., Staba, R.J., Andrillon, T., et al. (2011) Regional slow waves and spindles in human sleep. Neuron, 70(1): 153–169.
[10] American Academy of Sleep Medicine. (2023) Sleep stages and scoring overview. Available from: https://aasm.org/resources/scoringmanual/
[11] Delorme, A., Makeig, S. (2004) EEGLAB: an open source toolbox for analysis of single-trial EEG dynamics. J Neurosci Methods, 134(1): 9–21.
[12] Welch, P. (1967) The use of fast Fourier transform for the estimation of power spectra. IEEE Trans Audio Electroacoustics, 15(2): 70–73.
[13] Kruskal, W.H., Wallis, W.A. (1952) Use of ranks in one-criterion variance analysis. J Am Stat Assoc, 47(260): 583–621.
[14] Mann, H.B., Whitney, D.R. (1947) On a test of whether one of two random variables is stochastically larger than the other. Ann Math Stat. 18(1): 50–60.
[15] Tononi, G., Cirelli, C. (2006) Sleep function and synaptic homeostasis. Sleep Medicine Reviews, 10(1): 49–62.